Anti-Stokes luminescence cooling of Tm^{3+}doped BaY_2F_8

Wendy Patterson[1], Stefano Bigotta[2], Mansoor Sheik-Bahae[1], Daniela Parisi[2], Mauro Tonelli[2], and Richard Epstein[3]

[1]*Optical Science and Engineering Program, Department of Physics and Astronomy, University of New Mexico, Albuquerque, NM 87131*

[2]*INFN - Sez. di Pisa, Largo B. Pontecorvo 3, 56127 Pisa, Italy*
NEST - Scuola Normale Superiore, Piazza dei Cavalieri 7, 56126 Pisa, Italy

[3]*Los Alamos National Laboratory, Los Alamos, NM 87545*
msb@unm.edu

http://www.optics.unm.edu/sbahae/

Abstract: We report laser-induced cooling with thulium-doped BaY_2F_8 single crystals grown using the Czochralski technique. The spectroscopic characterization of the crystals has been used to evaluate the laser cooling performance of the samples. Cooling by 3 degrees below ambient temperature is obtained in a single-pass geometry with 4.4 Watts of pump laser power at λ = 1855 nm.

OCIS codes: (140.3320) Laser cooling; (160.5690) Rare-earth-doped materials; (140.3380) Laser materials; (300.6280) Spectroscopy, fluorescence and luminescence; (160.1190) Anisotropic optical materials.

References and links

1. *Laser Cooling of Solids*, edited by Richard I. Epstein, Mansoor Sheik-Bahae, Proc. SPIE **6461** (Bellingham, Washington, 2007).
2. R.I. Epstein, M.I. Buchwald, B.C. Edwards, T.R. Gosnell, C.E. Mungan, "Observation of laser-induced fluorescent cooling of a solid," Nature **377**, 500–502 (1995).
3. J. Thiede, J. Distel, S.R. Greenfield, R.I. Epstein, "Cooling to 208 K by optical refrigeration," Appl. Phys. Lett. **86**, 154107 (2005).
4. M. Sheik-Bahae, R. Epstein, "Can laser light cool semiconductors?," Phys. Rev. Lett. **92**, 247403 (2004).
5. C.W. Hoyt, M. Sheik-Bahae, R.I. Epstein, B.C. Edwards, J.E. Anderson, "Observation of anti-Stokes fluorescence cooling in thulium-doped glass," Phys. Rev. Lett. **85**, 3600–3603 (2000).
6. J. Fernandez, A. J. Garcia-Adeva, R. Balda, "Anti-Stokes laser cooling in bulk erbium-doped materials," Phys. Rev. Lett. **97**, 033001 (2006).
7. S. Bigotta, D. Parisi, L. Bonelli, A. Toncelli, M. Tonelli, A. Di Lieto, "Spectroscopic and laser cooling results on Yb^{3+}-doped BaY_2F_8single crystal," J. Appl. Phys. **100**, 013109 (2006).
8. J.M. Parker, Annu. Rev. Mater. Sci. "Fluoride glasses," **19**, 21–41 (1989).
9. C.W. Hoyt, M. Sheik-Bahae, M. Ebrahimzadeh, "High-power picosecond optical parametric oscillator based on periodically poled lithium niobate," Opt. Lett. **27**, 1543–1545 (2002).
10. C.W. Hoyt, M.P. Hasselbeck, M. Sheik-Bahae, R. Epstein, S. Greenfield, J. Thiede, J. Distel, J. Valencia, "Laser cooling in thulium-doped glass," J. Opt. Soc. Am. B **20**, 1066–1074 (2003).
11. F. Cornacchia, D. Parisi, C. Bernardini, A. Toncelli, and M. Tonelli, "Efficient, diode-pumped Tm^{3+}:BaY_2F_8vibronic laser," Opt. Express **12**, 1982–1989 (2004).
12. R. I. Epstein, J. J. Brown, B. C. Edwards and A. Gibbs, "Measurements of optical refrigeration in ytterbium-doped crystals," J. Appl. Phys. **90**, 4815–4819 (2001).

#88918 - $15.00 USD Received 23 Oct 2007; revised 28 Nov 2007; accepted 29 Nov 2007; published 24 Jan 2008

13. K. Puech and L. Lefort and D. C. Hanna, "Broad tuning around degeneracy in a singly resonant synchronously pumped parametric oscillator by means of a diffraction grating," J. Opt. Soc. Am. B **16**, 1533–1538 (1999).

1. Introduction

Laser cooling of solids is receiving increased attention because it can be the foundation of compact, rugged, efficient, and reliable cryo-coolers [1]. This concept — sometimes referred to as optical refrigeration — uses anti-Stokes fluorescence to remove thermal energy from a condensed matter system, thereby reducing its net temperature. A laser beam excites the material in its low energy absorption tail, i.e. below the mean fluorescence photon energy, ν_f. Optical excitations thermalize with the lattice by absorbing phonons; these excitations then recombine at wavelengths blue-shifted from the pump light, with a cooling efficiency of $\eta_c = (\nu - \nu_f)/\nu$.

The first experimental demonstration was made in 1995, in which a cw titanium sapphire laser (λ = 1015 nm) pumped Yb^{3+}atoms doped in a heavy-metal-fluoride glass (ZBLAN) leading to a net temperature reduction of about 0.3 degrees [2]. The cooling record has since been pushed to an absolute temperature of 208 K using Yb^{3+}:ZBLAN corresponding to a temperature drop of $\sim$ 88 degrees below the ambient [3]. Laser-cooled solids have now entered the temperature regime of high-performance thermoelectric coolers, with the potential to attain cryogenic temperatures. It has been predicted that laser-cooling of direct-gap semiconductors such as GaAs may allow realization of absolute temperatures approaching 10 K [4].

There has been an ongoing effort to explore other rare-earth dopants and hosts because they can have advantages compared to Yb^{3+}:ZBLAN glass. Early work focused on Yb^{3+}-doped glasses and crystals due the small excited-state absorption. An important milestone was the observation of laser cooling in the presence of excited state absorption using Tm^{3+}:ZBLAN [5]. The Tm^{3+}:ZBLAN material system also provides an approximate two-fold increase in quantum efficiency, which scales inversely with excitation energy. Largely due to its inherently higher efficiency, Tm^{3+}:ZBLAN holds the current record for cooling power (i.e. radiative heat lift) of $\sim$ 70 mW. In 2006, laser cooling of an erbium-doped KPb_2Cl_5 crystal and CNBZn glass was reported [6]. This is a significant result because the cooling transition in erbium is accessible to high-power laser diodes.

Here, we present results from laser cooling experiments with Tm^{3+}-doped BaY_2F_8. To the best of our knowledge, this is the first time a Tm^{3+}-doped single crystal showed net cooling. This crystalline host offers many important advantages compared to ZBLAN that make it attractive for laser cooling applications [7]. First, it has lower phonon energy (45 meV compared to 72 meV) which reduces the rate of deleterious non-radiative decay via a multi-phonon emission pathway. This leads to higher quantum efficiency. It also has greater transparency at thermal wavelengths (far-infrared) that make it less susceptible to radiative heat loading. We estimate the emissivity to be $\varepsilon \approx 0.77$ compared to 0.89 for ZBLAN. Additionally, the thermal conductivity is $\sim$ 7 times higher than ZBLAN. A fourth advantage we note is the higher material hardness of the BaY_2F_8 host which allows for better polish and direct deposition of optical coatings. Moreover, it is significantly less hygroscopic than ZBLAN [8]. The Stark splitting in the ground state manifold is greater than Tm^{3+}:ZBLAN, which limits the absolute minimum achievable temperature, but has the advantage of increasing efficiency at room temperature. Although BaY_2F_8 has less favorable conductivity and hardness compared to the widely used YAG laser crystal, its superior optical properties and quantum efficiency make it a better choice for laser cooling [7].

#88918 - $15.00 USD Received 23 Oct 2007; revised 28 Nov 2007; accepted 29 Nov 2007; published 24 Jan 2008

2. Experimental

2.1. Crystal growth

Crystal growth was carried out at the Physics Department of the University of Pisa in a Czochralski furnace with resistive heating. With this apparatus, BaY_2F_8 single-crystals with nominal doping of 1.2% thulium have been grown by adding suitable amounts of $BaTm_2F_8$. To avoid OH^{-1} contamination, the fluoride starting materials are purified at AC Materials (Orlando, FL) and the growth process carried out in a high-purity (99.999%) argon atmosphere. During growth, the rotation rate of the sample is 5 rpm, the pulling rate 0.5 mm/h, and the temperature of the melt is in the range 987-995 °C. The furnace is also equipped with a computer-controlled apparatus for diameter control. The average size of the BaY_2F_8 crystals was about 15 mm in diameter and 55 mm in length. The crystals are of good optical quality and appear to be free of cracks. The crystals were analyzed using the X-ray Laue technique, verifying their monocrystalline structure and crystallographic axis orientation. The crystals are cut in small samples with edges along *b* and *c* axes because they are the most important orientations for optical applications. The faces are polished to high optical quality using alumina suspensions.

2.2. Spectroscopic set-up

The measurement of the room temperature absorption coefficient has been performed by means of a spectrophotometer (*VARIAN CARY 500 Scan*) operating in the range 250–3200 nm, with typical resolution near 0.1 and 1 nm in the visible and in the NIR, respectively. The room temperature fluorescence spectra of the $^3F_4 \rightarrow {}^3H_6$ transition were performed with the aim to measure the mean fluorescence wavelength (λ_f) and to derive a better estimate for the absorption coefficient in the long wavelength tail of the absorption spectra. The pump source was a tunable cw Ti:Al_2O_3 laser, pumped by an Ar^+ laser. The fluorescence signal is detected perpendicular to the pump laser direction to avoid spurious pump scattering. The luminescence was chopped then focused by a monochromator with 25 cm focal length, equipped with a 300 gr/mm grating; the resolution of the measurement was 1.2 nm. To record the spectra in various sample orientations, a Glan-Thomson polarizer is placed in front of the input slit of the monochromator. The signal was filtered by a silicon filter, detected by a liquid nitrogen cooled InSb detector, fed into pre-amplifiers, processed by a lock-in amplifier and subsequently stored on a PC.

2.3. Laser cooling

We excited the sample using a high power, singly-resonant, optical parametric oscillator (OPO) based on periodically-poled $LiNbO_3$ [9]. The OPO is synchronously pumped by 80 ps (FWHM) mode-locked pulses from a Nd^{3+}:YAG laser at a wavelength of 1.064 μm with a repetition rate of 76 MHz, delivering up to 20 W. The OPO output is tunable between 1.7–2.1 μm with power in the range of 4–6 Watts. However, when the OPO is operating at high power and near degeneracy (2.128 μm), there is a tendency towards several resonant oscillations, together with the undesirable features of frequency and mode instability [13]. As a result, the signal bandwidth can be as large as tens of nanometers. The insertion of two etalons within the OPO cavity significantly stabilized and reduced the bandwidth of the signal radiation to within the limitations of the spectrometer ($\approx$ 1 nm). The room temperature reference sample is placed in a vacuum chamber ($\sim 10^{-5}$ Torr) suspended by two glass microscope slides in order to minimize heat load from thermal conduction. The pump light makes a single pass through the sample. The change in temperature is measured relative to the reference sample using a micro-bolometer camera (Raytheon 2000AS) which views the sample through an IR-transparent window (NaCl). The camera was calibrated against a precision silicon temperature diode in a separate measurement

#88918 - $15.00 USD Received 23 Oct 2007; revised 28 Nov 2007; accepted 29 Nov 2007; published 24 Jan 2008

by placing the sample in a variable temperature cryostat. The data were stored by a frame-grabber card on a PC as 8-bit pixel image files.

3. Spectroscopic and cooling results

BaY_2F_8 is a biaxial crystal, and therefore requires six spectra to be fully characterized. Transitions between $^3F_4 \rightarrow {}^3H_6$ levels in Tm^{3+} ions, however, are dominated by the electric-dipole term and, as a result, it is not necessary to take the orientation of the magnetic field into account. Additionally, the polarized spectroscopic properties of Tm^{3+}doped BaY_2F_8 are readily available in the literature [11]. For the aim of this work, it is sufficient to show the spectroscopic measurements carried out along the $E \parallel b$ polarization, i.e. the one used for our laser cooling experiments, even if we used all three polarization components in order to derive the mean fluorescence wavelength, λ_f. Luminescence and absorption data for Tm^{3+}:BaY_2F_8 are shown in Fig. 1, which displays appreciable absorption at wavelengths longer than λ_F = 1793 nm (shaded region to the right of the solid vertical line). The presence of absorption beyond λ_F (by at least kT) is a key requirement for cooling. We note that crystalline hosts exhibit sharper spectral features, as compared to amorphous materials, due to the regular periodic structure of their atoms. These larger peaks in the target absorption region can be used advantageously in a laser cooling experiment.

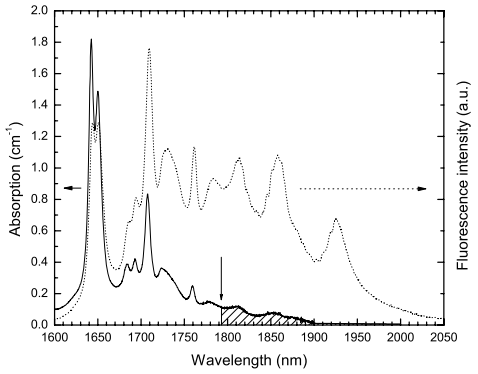

Fig. 1. $E \parallel b$ absorption (solid curve) and emission (dotted curve) spectra for our 1.2% Tm^{3+}:BaY_2F_8 sample. The solid vertical line indicates the mean fluorescent wavelength at λ_F = 1793 nm. In a laser cooling experiment, excitation takes place on the long wavelength side of this line in the shaded absorption region.

In order to exactly predict the expected temperature drop and determine the cooling efficiency, the value of the absorption coefficient in the long-wavelength tail must be known with high precision. Given that the absorption coefficient in the region of interest for laser cooling applications is usually very small when obtained using transmission spectroscopy, it is common practice to derive the absorption coefficient from the emission spectra using a reciprocity relation [12].

Generalizing the expression found in the cited work for the case of anisotropic crystals, we obtain:

$$\sigma_{abs}^{\gamma} = \frac{Z_u}{Z_l} \quad \sigma_{em}^{\gamma} \exp\left[\left(\frac{hc}{\lambda} - E_{ZPL}\right)/kT\right] \propto \lambda^5 I^{\gamma}(\lambda) e^{hc\lambda/kT} \tag{1}$$

#88918 - $15.00 USD Received 23 Oct 2007; revised 28 Nov 2007; accepted 29 Nov 2007; published 24 Jan 2008

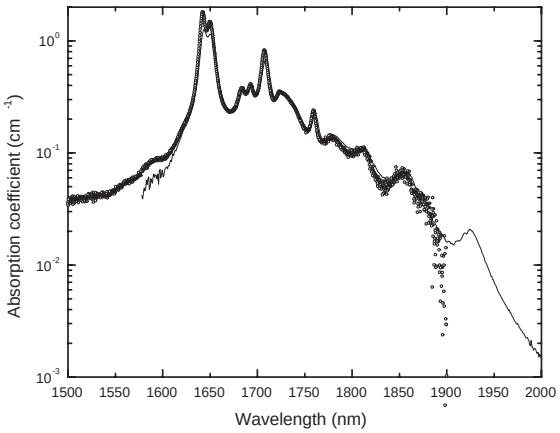

Fig. 2. $E \parallel b$-polarized absorption spectrum of 1.2% Tm^{3+}:BaY_2F_8. The open circles represent the data obtained with the spectrometer, while the solid line indicates the absorption derived from the emission spectrum using the reciprocity relation shown in the text.

where σ_{abs}^{γ}, σ_{em}^{γ} and $I^{\gamma}(\lambda)$ are the absorption and emission cross sections and the intensity of the fluorescence emission for the γ polarization; Z_u and Z_l are the partition functions for the upper and the lower electronic levels and E_{ZPL} is the energy of the zero phonon line. The values obtained by inserting the emission intensity data (normalized to the spectrometer absorption coefficient at large absorption) were over an order of magnitude above the noise level of our instrument. As shown in Fig. 2, the data obtained from reciprocity are in excellent agreement with those acquired with the spectrometer, and they give a better signal-to-noise ratio for $\alpha < 10^{-1}$ cm^{-1}. The discrepancy between the two curves at the largest peak (1650 nm) can be easily ascribed to the reabsorption process which decreases the luminescence intensity and hence the inferred absorption coefficients.

The change in temperature (relative to a reference sample) is recorded as a function of time for a given pump wavelength, and subsequently fitted to a single exponential decay, whereby the maximum temperature change at a given pump wavelength can be inferred. On average, a sample will take approximately 40 minutes to reach its equilibrium cooling or heating state. This wavelength-dependent temperature change (ΔT) normalized to pump power (P) is shown in Fig. 3 for the $E \| b$ orientation of the crystal. We correlate the two minima at $\sim$1850 and $\sim$1925 nm with the presence of absorption peaks around these wavelength for the $E \| b$ polarization. This experimental data is analyzed quantitatively by fitting with the following relation [5]:

$$\frac{\Delta T}{P} \sim \kappa \left[\alpha_B + \alpha_R(\lambda)\,(1-\eta_q) - \alpha_R(\lambda)\eta_q \frac{\lambda - \lambda_F}{\lambda_F} \right] \tag{2}$$

where α_B is the wavelength-independent background absorption coefficient, $\alpha_R(\lambda)$ is the resonant absorption data shown in Fig. 2, η_q is the non-unity quantum efficiency coefficient to account for deleterious fluorescence quenching, and κ takes into account the geometry of the sample and the vacuum chamber as well as thermo-dynamic factors (i.e. the radiative heat transfer). The constant coefficients η_q and α_B and κ are adjusted to fit the heating/cooling data. We

#88918 - $15.00 USD Received 23 Oct 2007; revised 28 Nov 2007; accepted 29 Nov 2007; published 24 Jan 2008

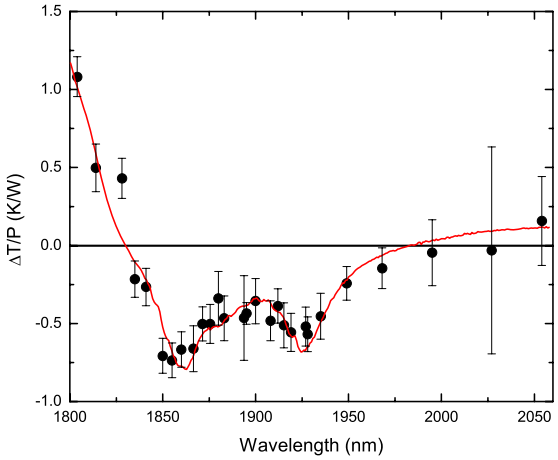

Fig. 3. Wavelength-dependent temperature change normalized to pump power for BaY_2F_8 doped 1.2% Tm^{3+} for $E \| b$. Data points below the horizontal reference line indicate net cooling. The solid curve is a fit as described in the text.

find $\eta_q \approx 0.98$, $\alpha_B \approx 2 \times 10^{-4}$ cm^{-1} for $E \| b$ and $\kappa = 723$ cmK/W for the data presented in Fig. 3. It is worth noting that the experimental value of κ is lower than the theoretical value. This can be ascribed to stray light circulating in the vacuum chamber due to the spurious reflections of the pump beam which can inadvertently heat the sample. A more refined pumping scheme could reduce the spurious reflections inside the vacuum chamber and hence enhance the cooling efficiency. Our configuration produced a maximum temperature drop of 3.2 degrees, at a wavelength of 1855 nm, given 4.4 W of pump power.

For practical applications, an estimate of the cooling efficiency, i.e. the ratio of the absorbed and the cooling power, is crucial. The absorbed power can be easily estimated using the Lambert-Beer law:

$$P_{abs} = P_{in}(1 - e^{-\alpha \ell}) \tag{3}$$

where ℓ is the length of the crystal, α is the total absorption coefficient and P_{in} is the incident power on the sample. The cooling power can be obtained from general thermodynamical considerations. In fact, at equilibrium the cooling power must balance the incoming power. If we consider that the only heat load on the sample is due to the radiation from the vacuum chamber, we can write:

$$P_{cool} = P_{heat} = \varepsilon_s \sigma A (T_c^4 - T_s^4) \tag{4}$$

where T_s is the temperature of the sample, T_c is the vacuum chamber temperature, ε_s is the emissivity of the host material, A is the surface area of the sample, and σ is the Stefan-Boltzmann constant. The cooling efficiency, η_{cool}, is then obtained by dividing Eq. 4 by 3. Shown in Fig. 4 are both the theoretical and the experimental cooling efficiency versus pump wavelength for the 1.2% Tm^{3+}:BaY_2F_8 crystal when pumped in the $E \parallel b$ polarization. A maximum cooling efficiency of $\eta_{max} = 3.4\%$ has been observed at 1934 nm. The slope attained at λ = 1855 nm is -0.74 deg/Watt which compares favorably to the best previously reported values of η_{max} = 3% and –0.73 deg/Watt for Tm^{3+}:ZBLAN [10]. The discrepancy between the theoretical and experimental data at wavelengths longer than $\sim$ 1950 nm can be ascribed to the low absorption coefficient in this region (hence, the large error bars).

#88918 - $15.00 USD Received 23 Oct 2007; revised 28 Nov 2007; accepted 29 Nov 2007; published 24 Jan 2008

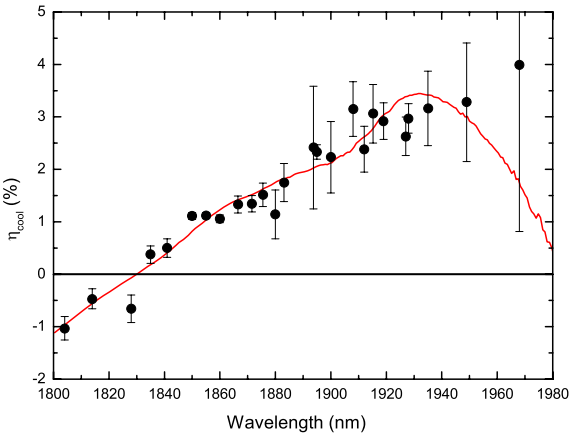

Fig. 4. Cooling efficiency as a function of the pump wavelength for the 1.2% Tm^{3+}-BaY_2F_8 crystal. The theoretical prediction (solid line) and experimental data (dots) are shown for $E \parallel b$.

Note that the maximum cooling efficiency occurs at 1934 nm, while the maximum temperature drop occurs at 1855 nm. In the ideal case with no impurities, η_{cool} increases with increasing wavelength [2]. This is clearly visible in Fig. 4 for wavelengths up to 1934 nm, beyond which the impurity absorption dominates and the cooling efficiency decreases. According to Eq. 2, the temperature drop for a given pump power is proportional to the product of α_R (Fig. 2) and η_{cool} (Fig. 4). Since with increasing wavelength, α_R decreases and η_{cool} increases, $\Delta T/P$ (Fig. 3) forms a minimum which is found at 1855 nm.

A similar analysis was performed also for the $E \perp b,c$ polarization. The results, not shown here, are comparable with that observed for the $E \parallel b$ polarization and are in good agreement with theoretical values.

4. Conclusion

In summary, we report the first observation of laser cooling with Tm^{3+}:BaY_2F_8. This crystalline host has shown net cooling when doped with the rare-earth ions Yb^{3+} and Tm^{3+} which allows for pumping at distinctly different wavelengths. BaY_2F_8 possesses a range of properties that compare favorably with ZBLAN glass in laser cooling applications.

This work was funded by a Multi-disciplinary University Research Initiative (Consortium for Laser Cooling in Solids) sponsored by the Air Force Office of Scientific Research (Grant FA9550-04-1-0356) and Air Force Grants F49620-0201-0059 and F49620-02-1-0057. W. Patterson acknowledges support of a National Science Foundation IGERT Fellowship. We thank J. Thiede for sample polishing and M.P. Hasselbeck for proofreading the manuscript, and F. Cornacchia and A. Toncelli for useful discussions.

#88918 - $15.00 USD Received 23 Oct 2007; revised 28 Nov 2007; accepted 29 Nov 2007; published 24 Jan 2008